



AIAA-2001-2985

**PROGRESS TOWARDS A REAL-TIME
QUANTITATIVE MEASUREMENT TECHNIQUE FOR
HIGH-SPEED FLOWS**

**Brian Thurow, James Hileman, Mo Samimy and Walter
Lempert**

**THE OHIO STATE UNIVERSITY
Department of Mechanical Engineering
Columbus, OH 43210**

**31st AIAA Fluid Dynamics Conference and
Exhibit**

June 11 - 14, 2001/ Anaheim, CA

PROGRESS TOWARDS A REAL-TIME QUANTITATIVE MEASUREMENT TECHNIQUE FOR HIGH-SPEED FLOWS

B. Thurow*, J. Hileman*, M. Samimy†, W Lempert‡

Gas Dynamics and Turbulence Laboratory

Dept. of Mechanical Engineering

The Ohio State University

The development of a new technique, termed real-time planar Doppler velocimetry (RTPDV), is explored. The technique is based upon planar Doppler velocimetry (PDV), which measures velocity components across a plane and has been developed and used for the past 10 years. The new technique incorporates recent technological advances in laser and camera systems. A series of experiments was designed to test the effectiveness of the new components in the system. An iodine filter profile was obtained by scanning a home built pulse burst laser through a range of frequencies and measuring the transmission of laser light through the filter. The laser was found to operate between 18787.0 cm^{-1} to 18789.5 cm^{-1} . Using the pulse burst laser and a commercially available 10 Hz Nd:YAG laser to form a spot on a stationary sheet of paper, the relative effectiveness of the laser and experimental system was explored. Due to the experimental set-up, preliminary images captured by the ultra-fast camera seemed to be dominated by ‘speckle’ noise. The pulse-burst laser is shown to have a better frequency stability than the commercial laser, but is limited by its lower power. Cursory experiments conducted on a high-aspect ratio Mach 2.0 rectangular jet indicate the technique’s potential, but also draw attention to key challenging issues to be reckoned with.

I. Introduction

Experimental techniques in fluid flows are continuously being pushed to their limits as researchers strive for more and more detailed information. As computers increase in power, researchers are looking for high quality quantitative experimental data in order to improve the accuracy of large eddy simulations (LES) and direct numerical simulations (DNS) towards predicting these flows.

Traditionally, measurements are divided into two categories, intrusive and non-intrusive. Intrusive measurements, such as pitot probes and hot-wires can provide accurate measurements, but lack spatial resolution. Spatial information can be obtained by having multiple probes in the flow but is quite limited by the finite size of the probes. Furthermore, intrusive measurements, by their very nature, disturb the flow and are largely restricted by this.

A large class of non-intrusive optical diagnostic techniques has been developed that do not have the same limitations. Techniques such as schlieren and shadowgraph can provide high spatial resolution of the density gradients within flows, but are limited by the line-of-site integration associated with them. More recently, researchers have begun using

lasers to interrogate the flow. Techniques using lasers, such as laser Doppler velocimetry (LDV), have been able to replace many of the traditionally used probe techniques and new techniques have been created which greatly advance upon previously available techniques.

One particular technique that has emerged in the last decade or so is planar Doppler velocimetry (PDV). PDV has the ability to measure all three components of velocity over a plane in the flow created by a laser sheet. PDV utilizes the frequency shift of laser light after it is scattered by a moving particle. Similar to planar imaging velocimetry (PIV), the technique yields an instantaneous snapshot of the velocity field within a given flow field. The spatial resolution is unmatched by any other existing technique.

Researchers have realized the potential benefits of PDV and have developed it over the last decade into a viable and reliable non-intrusive technique. Despite the successes to this point with PDV, the technique will ultimately be limited by its lack of temporal resolution. An ideal technique would measure velocity globally through the flow with resolution both in time and space. While the technology does not yet exist to realize this ideal, new technology has become available which will allow for the velocity of flows to be measured both in space and time over a short period of time.

* Graduate Student, AIAA Member

† Professor, AIAA Associate Fellow; Corresponding author

‡ Associate Professor, AIAA Associate Fellow

This technique, currently termed real-time PDV (RTPDV), aims to utilize recent advancements in laser and camera technologies to provide real-time information using the PDV technique as its basis. While the technique is still in its early developmental stages, this paper details the initial progress that is currently being made to make RTPDV a reality.

II. Planar Doppler Velocimetry

The basic concept of PDV is relatively straightforward and simple. When light at a given frequency, f , is scattered by a moving particle it experiences a frequency shift, Δf_d , that is proportional to the velocity of the particle. The fundamental equation of PDV, the Doppler shift equation, is:

$$\Delta f_d = \frac{(\vec{s} - \vec{o}) \cdot \vec{V}}{\lambda} \quad (1)$$

where s is the unit vector in the direction of the scattered light, o is the unit vector in the direction of the incident laser light, λ is the wavelength of the light and V is the velocity of the particle.

In practice, the frequency shift cannot be directly measured. Rather, a molecular filter is used as a frequency discriminator. In typical PDV applications a molecular filter consists of a glass cell filled with iodine. Due to the rotational and vibrational molecular transitions of iodine gas, the transmission of light through the cell is a function of the light's frequency, the gas pressure and the gas temperature. Therefore, the frequency shift of light can be determined by measuring the transmission of the scattered light as it passes through the filter. A simple schematic of this concept is found in Figure 1.

Figure 2 shows a schematic of a typical experimental set-up for PDV. A frequency-controlled laser is formed into a sheet and light scattered by particles contained in the flow. The image of the flow is then split into two using a beam splitter. The two images are directed along different paths with one path passing through a molecular filter. Both images are then recorded using a CCD camera. Some researchers use two cameras to record the filtered and unfiltered images, while others record both images on one camera by directing the light onto two different parts of the same CCD chip. The transmission of light intensity through the molecular filter will be a direct function of the light's frequency and, therefore, a measurement of the flow velocity at that point. The transmission is determined by comparing the filtered intensity to the non-filtered intensity.

This ratio of filtered and unfiltered light can be calculated for every pixel of the image. In order to do this, the two images must be precisely aligned and

mapped so that the intensity information from the filtered image corresponds to the exact same region of flow in the corresponding unfiltered image. This mapping is typically accomplished by placing a card with evenly spaced dots in line with the laser sheet. As the location of each dot is precisely known, the dots serve as 'tie' points between the two images. Each image is then processed to identify the locations of the dots in the image. The images are then mapped onto a new imaging plane determined by the locations of the dots in the original image. It has been determined that this mapping must be done to subpixel accuracy in order to get accurate velocity results.

Once the two images are mapped, a ratio for every point in the flow can be calculated assuming that each pixel has a uniform sensitivity to light intensity. In practice, each pixel on a given CCD chip has an independent 'gain' and 'bias' associated with it. Furthermore, as the filtered and unfiltered images travel through separate paths to the camera (or camera pair), variations in the two signals can arise. To account for these differences, the intensity of each pixel is examined with a known light source providing the images. The methods to accomplish this vary, but a typical procedure is to tune the laser to a frequency that fully transmits through the filter, and to illuminate a stationary plane with this light. After mapping the images, a 'gain' profile can be generated that results in equal intensities at the same point in each image when the light frequency is at full transmission. Following this procedure, the ratio of intensities at each point in the flow is calculated and consequently the frequency shift of the scattered light and therefore the velocity of the flow can be determined.

The key elements to PDV include the molecular filter, laser and camera. The literature concerning PDV and related technologies is quite extensive. Interested readers are directed towards comprehensive review articles by McKenzie [1996], Elliott and Beutner [1999] and Samimy and Wernet [2000]. The technique today has developed to the point where reliable velocity measurements with errors on the order of 2 m/sec can be readily obtained. Real-time PDV is a product of recent technological advances in both lasers and cameras. As such, it is important to understand the key characteristics of the lasers and cameras currently used by researchers in PDV applications.

Lasers Used in PDV

An ideal laser used in PDV would be able to produce short high-energy pulses of light with a very narrow spectral line width. The laser's frequency would be tunable so that the frequency could be readily and easily adjusted through the various

transmission/absorption transitions of the iodine filter. The typical laser used in PDV applications is a seeded Nd:YAG frequency-doubled pulsed laser. This laser has the ability to produce narrow-bandwidth, high-energy laser pulses and operates at 532 nm (green) wavelength. These lasers are pulsed in order to provide high instantaneous intensity. The repetition rate is thereby limited to the order of Hz due to thermal loading on the Nd:YAG gain medium. The laser's frequency is tunable and matches well to some strong absorption/transmission transitions in the iodine filter's spectrum.

Standard Nd:YAG lasers do not exhibit the narrow line width and frequency stability necessary for PDV. To remedy this, the lasers incorporate a seeding system whereby a narrow line width, low power continuous wave (cw) laser is introduced into the oscillating cavity. The amplified light then has nearly the same properties as the seed beam. For this to work, however, the length of the oscillating cavity must match a multiple of the seed laser's wavelength in order to achieve maximum gain. If the length of the cavity does not match, other frequencies of light will have a higher gain within the cavity and dominate the light output. To get around this, lasers typically use a piezoelectric actuated mirror to match the length of the cavity to the seed laser's wavelength. This arrangement has been successful in creating narrow line width laser pulses (<100 MHz).

The laser system is still prone to some problems that might interfere with accurate PDV results. As the frequency must be matched between the seed laser and the main oscillator of the system, the frequency characteristics of the laser can only be as good as the seed laser itself. Many seeder designs, however, also incorporate a linear oscillator whose length determines the frequency. This causes the seed frequency to be subject to frequency drift over time due to temperature changes. Furthermore, the cavity mirror dither used to match the main oscillator with the seed laser can cause pulse-to-pulse jitters in the laser frequency. The combination of long-term drift and the pulse-to-pulse jitter has required the incorporation of frequency monitoring into PDV systems in order to measure the instantaneous frequency of each pulse. It has also been noticed by some researchers that the frequency of the laser can vary within the beam itself. This is alleviated by only using the centermost portion of the beam where the frequency appears to be more stable.

We use two commercially available Nd:YAG lasers that meet the specifications required for PDV; one is a Spectra-Physics Quanta-Ray PRO-250-10 and another one is a Continuum Powerlite 8010. These lasers operate at 10 Hz and can produce 700 mJ, 9 nsec pulses at 532 nm. Without seeding, they have a line

width on the order of 30 GHz. In seeded mode, the line width is less than 90 MHz with modulations less than 10 MHz. Typical frequency shifts will be on the order of 1 GHz with the filter profile curve from full transmission to full absorption occurring over about 2 GHz or so.

Cameras Used in PDV

The ideal camera used for PDV would have a large and efficient CCD chip with high spatial resolution and dynamic range. High quantum efficiency of the conversion of photons to electrons would help alleviate the need for increased laser power and would help resolve low intensity scattering. An increased spatial resolution would make velocity measurements on smaller scales within the flow possible and a large dynamic range would make measurement of intensity ratios more accurate. Furthermore, due to a phenomenon called 'speckle', which is image noise due to the constructive and destructive interference of coherent laser light as it images on the CCD chip, larger physical pixel sizes would reduce the noise levels within the image.

Many different camera models fit the specifications for a good PDV camera. We currently use a scientific grade SpectraVideo camera produced by PixelVision. This camera utilizes a 16-bit 1024 x 1024 backlit CCD chip. The backlighting allows for quantum efficiency above 90%. Each individual pixel has a size of 24 microns. The overall repetition rate of the camera without any pixel binning is less than 1 Hz.

III. Real-Time Planar Doppler Velocimetry

In the last few years, some technological advances have been made in both laser and camera technology that have made possible a MHz rate imaging system. This MHz rate imaging system incorporates a pulse-burst Nd:YAG laser and a MHz frame-rate CCD camera. Used in conjunction with one another, these technologies have been used to visualize the flow of a Mach 1.3 axisymmetric jet [Thurow et al. 2000, 2001 and Thurow, 2001] and the boundary layer of a hypersonic flow over a cone [Wu et al., 2000]. Substituting this new technology into a PDV set-up should lead to real-time PDV. These technologies are discussed below.

Pulse-burst MHz Laser

The laser, illustrated schematically in Figure 3, is a home-built second generation system based on that described previously by Lempert et al. [1996, 1997], Wu et al. [2000], Thurow et al. [2000, 2001] and Thurow

[2001]. A continuous wave Nd:YAG ring laser serves as the primary oscillator, the output of which is pre-amplified in a double-pass, flashlamp-pumped, pulsed amplifier. The resulting, approximately 200 microsecond duration pulse is formed into a "burst" train using a custom, dual Pockel Cell "slicer", purchased from MEDOX electro-optics. The train can have a variable number of pulses, between 1 and 99, with inter-pulse spacing varying between 1 and 100 microseconds. The individual pulse durations can be variable between 5 nsec and 10 microseconds. In recently conducted experiments, a typical burst consisted of 17 pulses (limited by the camera), with 10 nsec duration and 2-10 microsecond spacing. The pulse train is further amplified by a pair of additional double-pass amplification stages and a single-pass, double-flashlamp, amplification stage. It is then converted to the second harmonic wavelength of 0.532 microns ("green") using a 6x6x8 mm KTP crystal.

Figure 4 shows a typical burst train, consisting of 17 pulses, each having duration of 10 ns. The inter-pulse spacing is 5 microseconds. The output energy, at the second harmonic wavelength (532 nm), is approximately 7 mJ in *each* of the individual pulses comprising the burst. Typical pulse energies vary between 2 and 10 mJ/pulse depending on the length of time between pulses. Figure 5 illustrates the effect of pulse separations on the total energy contained in a burst of 10 pulses. Longer separations between pulses correlate to higher pulse energies. Furthermore, the timing of the four amplifiers can be varied relative to one another in order to distribute the power evenly over the entire burst. The overall burst process has a repetition rate of 10 Hz.

In general, the laser is similar to the typical lasers used in PDV experiments, but there are a few key differences that should be discussed. First, the power in each pulse is approximately two orders of magnitude less than commercially available Nd:YAG lasers. This makes visualization of the flow much more challenging and will result in a lower signal to noise (S/N) ratio. Second, the pulse-burst laser does not incorporate any seeding. Rather, the laser is essentially a super-amplified seed laser. This has the strong advantage over typical systems in that any problems related to the frequency matching between the seed laser and the oscillation cavity are eliminated. Third, the main oscillator, which controls the frequency characteristics, uses a non-planar ring oscillator (NPRO) where the Nd:YAG material is formed into a unique crystal shape in which the amplified beam traverses. This design eliminates the 'spatial hole burning' associated with linear resonators that can lead to multimode operation. This allows all spatial modes to compete simultaneously for gain and thus forms a narrow line width beam. For operation at 1064 nm, this line width

is specified to be less than 5 kHz. This width is further broadened in the 10 nsec laser pulse due to the Fourier transform limit and is expected to be on the order of 60 MHz. The frequency of the laser is controlled by adjusting the temperature of the crystal and thus the spatial mode with the highest gain. This also leads to 'mode hopping'. As the temperature decreases, the frequency will slightly increase until a certain point where it will jump back slightly (mode hop). The long-term frequency drift is specified to be less than 50 MHz/hour.

Ultra-fast Digital Camera

The camera used in these experiments was manufactured by Silicon Mountain Design (SMD) (now a subsidiary of Dalsa, Inc.). The camera can acquire 17 images at a variable rate as fast as 1 MHz. Each image in the sequence has a resolution of 240 x 240 pixels. The camera is based on a large format (960 x 960) 12 bit CCD chip in which fifteen of sixteen pixels are hidden by a custom fabricated mask. By appropriate shifting of charge, individual images are initially stored in pixel locations under the mask. The seventeenth frame is obtained by using what is known as the CCD 'drain', which is normally used to dump dark charge collected in the interval between frames. After accumulation of all the images, a PC reads the output as one large image, containing all 17 frames. The output signal is transferred via four parallel data ports, each comprising a quarter size column of the image. The video signal out can have either a gain of 1 or 4 applied to it. Each pixel is 14 microns in size and the quantum efficiency is less than 20%.

In comparison with the scientific grade camera discussed earlier, the ultra-fast digital camera has a few drawbacks. First, the relatively small spatial resolution of 240 x 240 limits the spatial scale of measurements. This is compounded when using a single camera to record both the filtered and unfiltered images. Second, a pixel size of 14 microns is relatively small and should only serve to increase 'speckle' noise. Third, the low quantum efficiency necessitates a more intense signal. Compounded with the limited amount of available laser power, this should lead to a reduced S/N ratio and limit the scale of the flows on which experiments are being conducted. These issues will be discussed further.

Both the laser and camera have been used before in a flow visualization study of a Mach 1.3 axisymmetric jet [Thurow et al., 2000, 2001, Thurow 2001]. In these experiments, seed particles were introduced into the flow through product formation where water particles formed in the mixing layer of the jet as the warm, moist ambient air entrained and mixed with the cold and dry jet core air. The laser was formed into a sheet to illuminate various cross-stream and

streamwise planes of the jet. Figure 6 is an example of the results and demonstrates the capabilities of both the camera and the laser to perform the basic task of flow visualization. The nozzle exit diameter is 1" and the laser power was sufficient to illuminate between 4 and 6" of the flow.

IV. Experimental Set-up

Iodine Filter Profile

In order to investigate the capability of the laser to tune through certain frequencies, the laser was used to create a filter profile. A back reflection of the beam off of a right-angle turning prism was split into two using a 50/50 beam splitter. One of the beams was directed through an iodine cell and onto a photodiode. The other beam was also directed onto another photodiode. The two photodiode signals were then acquired using a pair of Stanford Research Systems boxcar integrators. Only the energy contained in the first pulse of the train of pulses was acquired. The laser's frequency was controlled by applying an offset voltage to the laser controller. This voltage was scanned from -10 V to +10 V in steps of 0.025 V and an average of 25 pulses was recorded for each step. There was a pause of at least 3 seconds between each step in order to allow the laser to reach its specified temperature. This procedure was performed on two separate days to get an idea about the long-term drift of the system. A theoretical profile was also obtained using a program provided by Innovative Scientific Solutions, Inc. (ISSI) based upon a code generated by Forkey [1996]. The iodine cell was prepared over three years ago with an iodine partial pressure of 4.28 torr and is pressure broadened with Nitrogen at 41 torr. The iodine cell is maintained at approximately 130 C.

Stationary Target Experiments

As a first test of a real-time PDV system, a PDV experiment was setup to measure the frequency shift of laser light scattering from a stationary target. This was thought to be an appropriate test as there should be no actual frequency shift and thus any measured shift will indicate what problems might lie within the system. A splitter/recombiner system was assembled next to the pulse-burst laser and was used to capture a filtered and unfiltered image on the camera CCD chip surface. The system is similar to the system depicted in Figure 2. The system uses a 50/50 beam splitter to create two images. Using mirrors, one image is directed through an iodine cell and onto one half of the camera. The other image is directed onto the other half of the camera. The camera was outfitted with a

zoom lens (f.l. from 70-210 mm, F/4-5.6). A 21 mm extension tube was needed in order to focus the camera at the desired location.

A dot card was created by using a laser printer and an overhead transparency. Each dot was roughly 1/32" in diameter and about 1/10" apart. The dot card was placed approximately 8" in front of the splitter/recombiner system. The path length through the splitter/recombiner system is roughly estimated to be 24". A white sheet of paper was placed behind the dot card and a portable 500-Watt lamp was used to illuminate the target. The camera lens was zoomed to about a 150 mm focal length and focused onto the dot card. After capturing an image of the dot card, the white sheet of paper was placed directly in front of the dot card and a large spot was formed using the laser and a -150 mm spherical lens. A compromise had to be made between the size of the spot and the intensity. The chosen spot size filled roughly half of the CCD chip but had a large enough intensity to have a distribution of intensities in the upper half of the available levels.

Based upon the results of the iodine filter profile to be discussed later, the laser was scanned from 1.0 to 2.0 volts in 0.02 volt increments. For each step, an average of 25 images was obtained. This was done in order to come up with a filter profile. Following this, the laser was set to 2.0 V, which corresponds to a point of maximum transmission through the iodine cell, in order to come up with a flat-field image. The laser power was adjusted to a variety of intensities through a combination of beam splitters and reduced power settings within the laser amplifiers controllers. A variety of images were then obtained at various power settings and spot sizes; each image was an average of at least 50. The camera's focus was not adjusted through this process.

Following this, the voltage to the laser was adjusted to 1.6 volts. This voltage corresponds to a region of maximum absorption through the filter. A stack of 50 images was then acquired in order to examine the shot-to-shot stability of the system. This process was then repeated at 1.70, 1.75 and 1.80 volts, which all correspond to different points along the filter profile.

For each image pair, a software package provided by Innovative Scientific Solutions, Inc. was used to condense and analyze the data. The software included routines to map the two images together and to calculate ratios and Doppler shifts. Each image was binned in 3 x 3 pixels.

The same exact procedure was then repeated using one of the commercial lasers described earlier in order to compare the two lasers. The commercial laser, which operates at a slightly different frequency than the pulse-burst laser, was tuned to a different location in the

iodine spectrum. The spot size was large enough to fill about 80 – 90% of the CCD chip and enough intensity to have values in the upper half of the available intensity levels.

Mach 2.0 High Aspect Ratio Rectangular Jet Experiments

A high aspect ratio Mach 2.0 rectangular half nozzle was designed and fabricated in order to provide a flow field for measurement using the real-time PDV system. A high-aspect ratio, rectangular nozzle was chosen as the flow is expected to be of a more two-dimensional quality than a circular or low-aspect ratio nozzle. A Mach 2.0 flow is relatively easy to seed due to the low temperatures produced by the expansion of the flow. Furthermore, the high speeds should induce a larger, and thus more easily measured, frequency shift. The dimensions of the nozzle were chosen to be 1/8" x 3/4". This creates a measurement volume that is large enough to be visualized using conventional optics, but small enough that the intensity of the laser sheet could be confined to a small region.

The converging-diverging nozzle contour was designed using the method of characteristics for uniform flow at the nozzle exit. Only one side of the nozzle is contoured while the other side of the nozzle contains a converging section to the nozzle throat and then straightens out, thus forming a half nozzle. The straight side of the nozzle has 0.032" hole at the center located 0.04" from the exit to measure the static pressure of the flow. The nozzle is connected to a 2" inner diameter stagnation chamber that is 4" in length. The chamber contains two screens of varying porosity to condition the flow and another pressure tap to measure the stagnation pressure. Air is supplied to the stagnation chamber from two four stage compressors; it is filtered, dried and stored in two cylindrical tanks with a total capacity of 42.5 m³ at 16.5 MPa (1600 ft³ at 2500 psi). Run times are virtually unlimited. The nozzle and stagnation chamber are positioned so that the nozzle flow exits vertically upwards and is approximately 8" from the splitter/recombiner set-up. The camera and filter set-up are located perpendicular to the streamwise and minor axis of the flow.

Seed particles are provided by small acetone droplets that form within the jet core. Acetone is injected through a spray nozzle approximately 15' upstream and evaporates by the time it reaches the nozzle. As the flow expands, the cold temperatures cause the acetone to condense into tiny droplets approximately 50 nm in size. This is small enough to follow the flow faithfully, but large enough to scatter the incident light.

A laser sheet was formed parallel with the minor axis of the jet. The sheet is angled at 14.6 +/- 0.3

degrees with respect to the streamwise direction, thus forming a quasi-streamwise view. The sheet propagated down and towards the camera. A 500 mm spherical lens and a -200 mm cylindrical lens were used to form the sheet. The camera was focused onto an area of about 1.6 x 1.6". This corresponded to a zooming focal length of 210 mm coupled with a 21mm extension tube. Figure 7 shows a picture of an experiment in progress. The laser beam is easily seen in the air due to an acetone mist resulting from seeding the jet with acetone. The nozzle is at the bottom of the picture and is being illuminated by the laser sheet, thus making it appear like a torch. The cage covered in black felt holds the splitter/recombiner optics and the camera. The geometry of the system results in a PDV system that is sensitive to the $0.968 i + 0.75 j + 0.00 k$ component of velocity, where i is the streamwise direction of the jet, j is along the major axis and k is along the minor axis.

V. Experimental Results and Discussion

Results at this point are very preliminary and must still be pondered before any definitive statements concerning the system can be made. The following results and discussion highlight the main issues concerning the development of RTPDV.

Iodine Filter Profile

Figure 8 is a plot of the transmission ratio obtained by changing the voltage applied to the master oscillator from -10 to +10 volts. Strong absorption and transmission bands are clearly seen. Many of the profile's features are repeated at various voltage inputs; this is a product of the 'mode hopping' discussed earlier. At points of higher transmission, the profile is not as well defined. This is possibly the result of a saturated photodiode or the transition between mode hops. It was later discovered that the energy in each laser pulse might be somewhat sporadic at certain settings in the laser equipment. While this should not affect the frequency of the laser pulses, it might lead to inconsistencies in the measurements. It is not clear whether the laser was acting in this manner during this set of experiments, but in subsequent experiments, laser settings were adjusted to avoid this phenomenon.

The data in Figure 8 was carefully examined to identify the locations of mode hops and the data subsequently condensed into a single filter profile. This is necessary in order to determine the sensitivity of the laser to input voltage in units of MHz/volt. A theoretical iodine profile was also examined in order to identify the various peaks and valleys of the spectrum. The condensed profile and the theoretical profile are

found in Figure 9. The two profiles match up fairly well with only minor differences. The program used to create the theoretical spectra had a limit imposed on the nitrogen pressure of 5000 Pa (37.6 torr) while the actual pressure was somewhat higher. This data indicates that the laser (second harmonic) can be tuned between 18787 cm^{-1} and 18789.5 cm^{-1} . This corresponds to a total range of about 75 GHz and an average tuning coefficient over the entire tuning range of 3.75 GHz/V. In between mode hops, the tuning coefficient is calculated to be 9.15 GHz/V. Figure 10 is a comparison of two profiles taken on two different days. A slight offset corresponding to less than 1 GHz is noticed, but the overall profile remains the same. This indicates that the laser frequency is fairly stable over long periods of time, but must still be checked before running a PDV experiment.

Stationary Target Experiments

Figure 11 shows a filter profile obtained using the PDV setup for the range of 1.00 to 2.00 V. The profile was obtained by taking the average ratio calculated for each image pair. This procedure appears to fairly accurately follow the contours of the filter profile obtained earlier and corresponds to the well located at 18788.4 cm^{-1} . The bumpy features on the bottom of the profile are thought to be a product of low laser power and an inefficient camera. The smooth bump in the center does match up well with the filter profile taken earlier, however. Figure 12 is an image of the ratio and a histogram of the values obtained at 1.80 V. It is reminded that 3 x 3 binning was applied. The image appears relatively noisy as also indicated by the wide spread of values in the histogram. The average ratio is 0.4518 and has a standard deviation of 0.1150 (25% of average). As the spot was formed on a stationary sheet of paper, the ratio at every point should theoretically be the same; therefore, the noise contained in the image is a concern.

One possible reason for the large amount of noise would be the phenomenon of ‘speckle’. Speckle has been a major concern for researchers conducting PDV experiments and is still not perfectly understood. An estimation for the noise-to-signal ratio (NSR) is given by Arsenault and April [1976] and Smith [1998]:

$$NSR = \lambda F / \Delta x \quad (2)$$

where λ is the wavelength of coherent laser light, F is the camera lens f -number and Δx is the average size of the camera pixels. Using an f -number of 5.6 and a pixel size of 14 microns, the NSR is estimated to be approximately 0.21. When compared to the NSR of 0.25 noticed in the image, it appears that ‘speckle’ noise is a large factor in the current experimental setup. The ‘speckle’ noise should have been somewhat reduced by the 3 x 3 binning used on the image. Unlike

conventional CCD cameras, however, the binning does not occur between adjacent pixels on the chip itself. It should also be noted that ‘speckle’ is not expected to be a function of the laser intensity. Although not included here for brevity, images acquired using the commercial laser also registered a high amount of noise. One such image has a NSR of 0.22. This indicates that the noise is most likely not a result of the laser used, but is most likely a product of the imaging optics and/or camera.

Other sources of noise might include the lack of proper image registration in the mapping procedure and the lack of a uniform light source for the flat field images. The flat field images were acquired by taking images of the stationary spot with the laser tuned to a full transmission region of the filter profile. Unfortunately, the beam shape had a diffraction pattern and was not increased large enough in size to fill the CCD chip. This might lead to inconsistencies in the calculation of the gain and offset associated with each pixel. Another contributing factor to the noise is the relatively low spatial resolution of the camera, which limits the amount of image processing that can be performed to remove noise and still maintain good spatial resolution.

Despite the presence of noise, the average ratio across an image should remain roughly the same from pulse to pulse. Any changes in the average from one pulse to the next would most likely be due to an actual frequency shift in the laser. Figure 13 shows the average ratio calculated for each image in a set of 50 images at different seed voltages for both the pulse-burst laser and the commercial laser. It should be noted that each ratio is calculated from the first pulse of the entire burst. Any differences between pulses within a single burst have not been examined at this time, but no significant differences are expected. At lower transmission levels, the measurement of the ratio varies quite a bit for the pulse burst laser (solid line) from shot to shot. This variation dramatically decreases at higher transmission levels. It is thought that at the lower transmission levels, the light passing through the filter is not of a high enough intensity to properly register on the relatively inefficient CCD. The commercial laser, having larger pulse energies, exhibits a smaller variation at low levels and demonstrates the limitations of the pulse burst laser’s low energy. At higher transmission levels, however, the two lasers perform rather equally with the pulse burst laser appearing to be more stable.

Taking a closer look at the two lines at a ratio of about 0.5 in Figure 13, the pulse-burst laser has an average ratio of 0.493 and standard deviation of 0.002 (0.4% of average) over the 50 ratios calculated. Conversely, the commercial laser has an average ratio of 0.541 and standard deviation of 0.026 (4.8% of average). The sporadic fluctuations contained within

the first 6 data points for the commercial laser are most likely due to the commercial laser losing seed. This is not unusual for these types of lasers and is one major reason frequency monitoring systems are commonly used. However, assuming that this is unusual and not typical of the laser, the pulse burst laser still appears to outperform the commercial laser. Neglecting the first six points for the commercial laser, the average ratio is 0.541 and the standard deviation is reduced to 0.007 (1.2% of average), but still fluctuates more than the pulse burst laser. These results seem to indicate that the pulse burst laser has better frequency stability from pulse to pulse than the commercial laser.

Preliminary results from the stationary target tests seem to indicate a few things. One, the NSR for the current experimental set-up is very high. This high ratio must be further examined. Further pixel binning might become necessary in the future, but the most dramatic change might result from the use of a lens with a smaller f -number. The overall imaging system must be more closely examined to locate the noise sources. Despite the large amount of noise, the tests indicate that the frequency characteristics of the pulse burst laser are ideal for PDV experiments. The burst-to-burst stability of the frequency appears to be at least a factor of 3 better than the commercial laser. For this reason, a frequency monitoring system is not deemed to be necessary in the immediate future, but might provide more accuracy down the road. The pulse burst laser, however, appears to suffer from a rather high NSR at lower transmission levels as the amount of signal passing through the filter is not large enough to accurately register on the camera. Any possible methods to boost the laser's output must be explored.

Mach 2.0 High Aspect Ratio Rectangular Jet

The data from experiments conducted on the Mach 2.0 jet are still being analyzed, but have yielded a limited amount of results so far. In conducting the experiments, it was attempted to acquire data by relying on the condensation of moisture from the ambient air entraining and mixing into the jet's mixing layer. Unfortunately, the intensity of the scattered light was not sufficient to yield any useful data. To increase the signal intensity, acetone was injected, evaporated and mixed into the flow upstream of the nozzle and condensed as the gas expanded through the nozzle. The addition of acetone proved to create a strong enough intensity to visualize the jet. A sample image taken is in Figure 14. The image is slanted due to the method in which the camera acquires and reads out the image. The left-hand side of the frame contains the unfiltered image while the right-hand side contains the filtered image. This figure demonstrates the ability of the system to capture both images on a single camera, but

also illustrates the limited amount of power available from the laser. The image is scaled from 0 to 140 intensity units out of a maximum of 4095. The spatial resolution of the camera also appears to be sufficient to make measurements on a variety of scales within the flow.

The large amount of noise present and the low intensity of the image made analysis of the data rather challenging. Instantaneous images are clearly contaminated with large amounts of noise and cover up many details about the flow. Despite these problems, the results should still indicate if the set-up is working in general. To determine this, the ratios calculated from one image pair was plotted on the histogram of Figure 15. This histogram also plots a reference point taken immediately afterwards on a stationary target. The seed voltage was kept constant at 1.7 volts, which corresponds to a laser frequency at which nearly full absorption occurs in the iodine spectrum. Two things are clear from this figure. One, the velocity of the Mach 2.0 flow is clearly causing a bulk Doppler shift. This shift in the peak is approximately 0.38. Referring to the profile of figure 11, this shift corresponds to a voltage on the curve of approximately 0.08 V, which subsequently corresponds to a bulk frequency shift of 732 MHz. Assuming that the bulk of the velocity is in the streamwise direction and referring back to equation 1, this finally translates into an average velocity on the order of 400 m/sec. Second, the histogram of values obtained with the jet on is much broader than the histogram obtained with no flow. The large spread is an indication of the various velocities being measured in the flow.

These results indicate that the PDV set-up incorporating the pulse burst laser and ultra-fast camera is detecting and measuring a Doppler shift of the light's frequency as it is scattered by particles in the flow. Currently, the images are dominated quite heavily by a large amount of noise thought to be the result of 'speckle'. Other sources of error might include problems with the image mapping and the flat field calibration.

VI. Conclusions

The fundamental concepts behind PDV were explored. The main components of PDV include a narrow spectral line width pulsed laser and a CCD camera. In current PDV set-ups, the repetition rate of both of these elements is limited to the order of Hz. The possibility of incorporating new advances in laser and camera technology should expand the current PDV technique into a real-time technique termed RTPDV. In regards to this possibility, the key elements of both technologies were examined and discussed.

A set of experiments was designed to make a first attempt to gather RTPDV data. The first experiment consisted of using the pulse burst laser to take an iodine filter profile. The experiment was successful and demonstrated the laser's single-frequency capabilities. The second experiment was designed to simulate a realistic RTPDV setup utilizing a stationary target as a known measurement volume. The set-up incorporated both the pulse burst laser and the ultra-fast camera. A commercial laser was also used for direct comparison with the pulse burst laser. Preliminary results show the presence of excessive image noise that is currently a large inhibiting factor in the measurement's capabilities. The relative inefficiency of the camera and low laser power will make measurements more challenging. Initial indications are that the pulse burst laser has better frequency stability than the commercial laser, thus eliminating the immediate need for a frequency

monitoring system. A third experiment using a Mach 2.0 rectangular nozzle was conducted to examine the effectiveness of the technique on taking measurements in an actual flow. While the results seem to be marred by the presence of image noise, the experiments at least provide an initial 'proof of concept' that the RTPDV has a future.

The main obstacle that currently stands in the way of RTPDV is image noise. The problem is further compounded by low laser power and a relatively inefficient camera. Future work will work to discover the main sources of this noise. Current speculation is that 'speckle' is the main contributor; less than ideal flat-field calibration and image mapping is also expected to contribute. Fortunately, 'speckle' is a well-studied problem with possible solutions available in the literature. Other work in RTPDV will include looking at mechanisms to increase laser power and possibly examining other available ultra-fast cameras.

Acknowledgments

The authors would like to thank NSF for their support of this research.

References

- Elliott, G., and Beutner, T., "Molecular Filter Based Planar Doppler Velocimetry," *Progress in Aerospace Sciences*, Vol. 35, 1999, pp. 799-845.
- Forkey, J.N., "Development and Demonstration of Filtered Rayleigh Scattering- a Laser Based Flow Diagnostic for Planar Measurements of Velocity, Temperature, and Pressure," Technical Report, Final Technical Report for NASA Graduate Student Researcher, Fellowship Grant #NGT-50826, Princeton University, 1996.
- Lempert, W. R., Wu, P. F., Zhang, B., Miles, R. B., Lowrance, J. L., Mastocola, V. J. and Kosonocky, W. F., "Pulse Burst Laser System for High-Speed Flow Diagnostics," AIAA Pap. 96-0179, 1996.
- Lempert, W. R., Wu, P. F. and Miles, R. B., "Filtered Rayleigh Scattering Measurements Using a MHz Rate Pulse-Burst Laser System," AIAA Pap. 97-0500, 1997.
- McKenzie, R.L., "Measurement Capabilities of Planar Doppler Velocimetry Using Pulsed Lasers," *Applied Optics*, Vol. 35, No. 6, 1996, pp. 948-964.
- Samimy, M., and Wernet, M. P., "Review of Planar Multiple-Component Velocimetry in High-Speed Flows," *AIAA J.*, Vol. 38, No. 4, 2000, pp. 553-574.
- Smith, M.W., "The Reduction of Laser Speckle Noise in Planar Doppler Velocimetry Systems," AIAA Paper 98-2607, June 1998.
- Thurow, B., Lempert, W. and Samimy, M., "MHz Rate Imaging of Large-Scale Structures within a High-Speed Axisymmetric Jet," AIAA Pap. 2000-0659, 2000.
- Thurow, B., Hileman, J., Samimy, M. and Lempert, W., "An In-Depth Investigation of Large Scale Structures in a Mach 1.3 Axisymmetric Jet," AIAA Pap. 2001-0148, 2001.
- Thurow, B., "Development and Application of a MHz-Rate Imaging System On the Visualization of Turbulence Structure in a Mach 1.3 Axisymmetric Jet," Master's Thesis, The Ohio State University, 2001.
- Wu, P., Lempert, W. R., and Miles, R. B., "MHz Pulse Burst Laser System and Visualization of Shock-Wave/Boundary Layer Interaction in a Mach 2.5 Wind Tunnel," *AIAA J.* **38** 672 (2000).

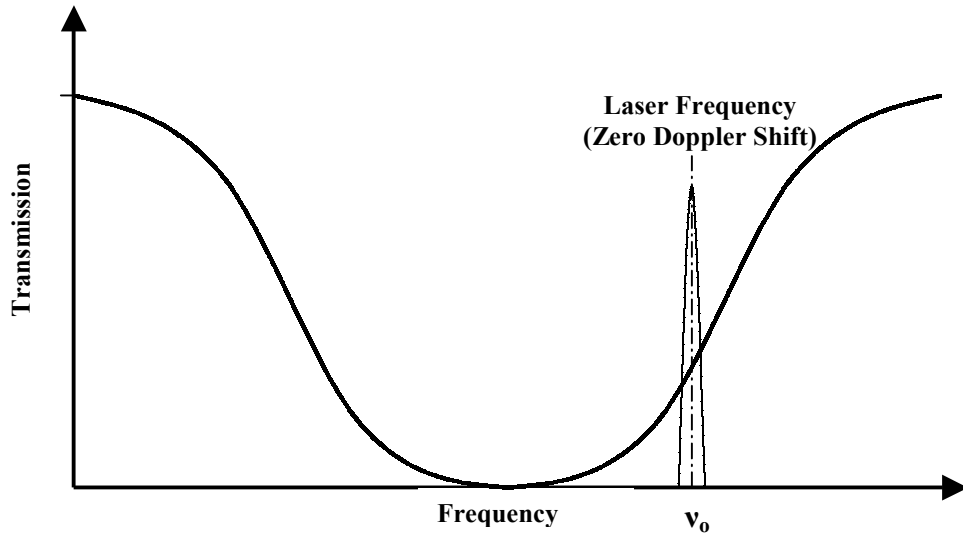


Figure 1 – Schematic of a molecular filter profile used with the PDV technique to measure Doppler shift.

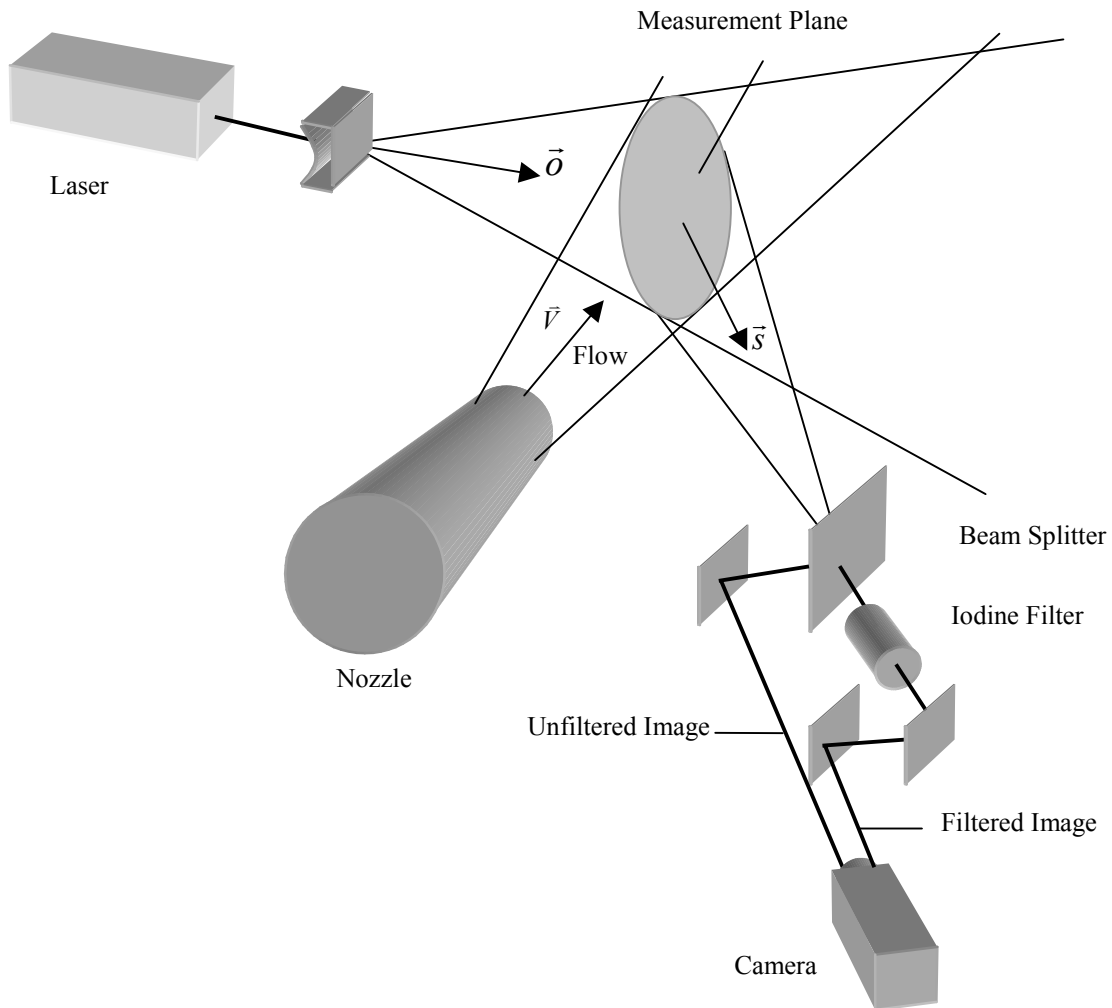


Figure 2 – Schematic of a one-camera, single-component PDV system. Taken from Samimy and Wernet [2000]

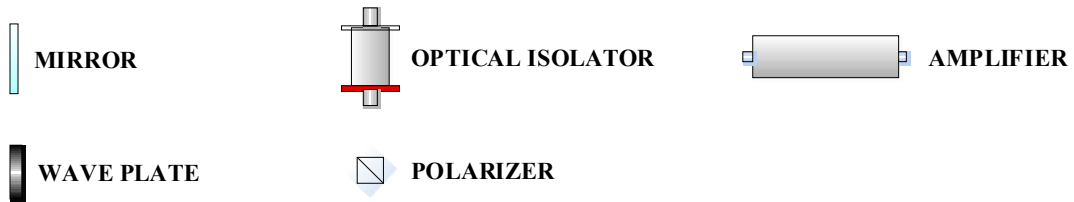
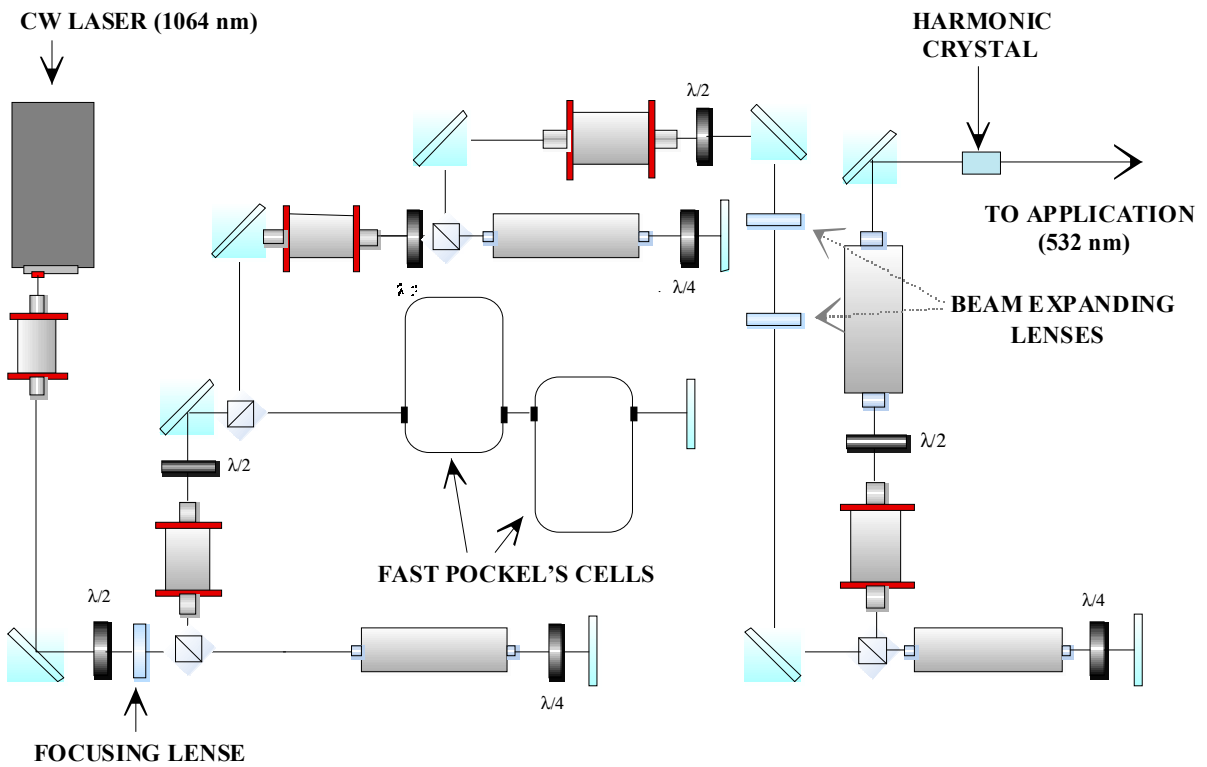


Figure 3 – Schematic of Pulse-Burst MHz Laser.

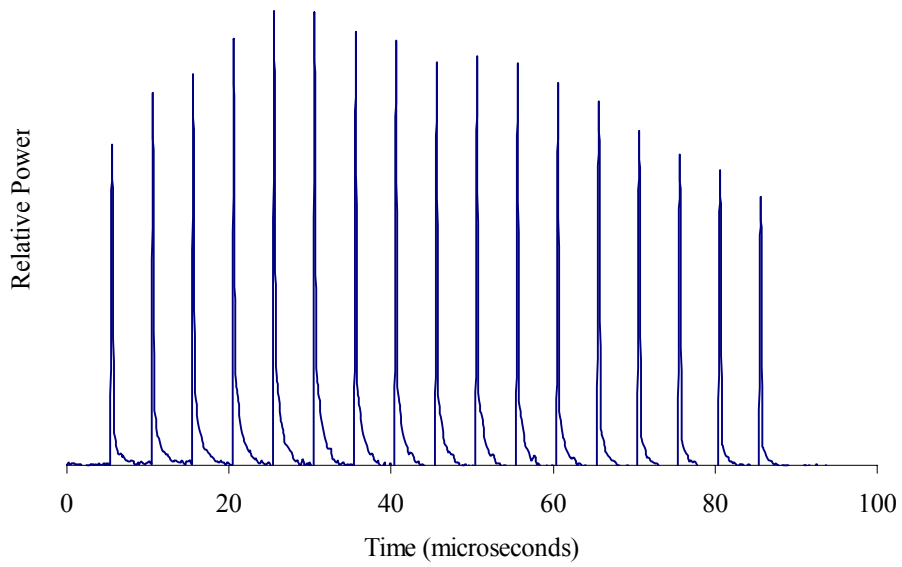


Figure 4 - Typical burst train for MHz Pulse Burst Laser; pulses are separated by 5 microseconds each and contain approximately 7 mJ each.

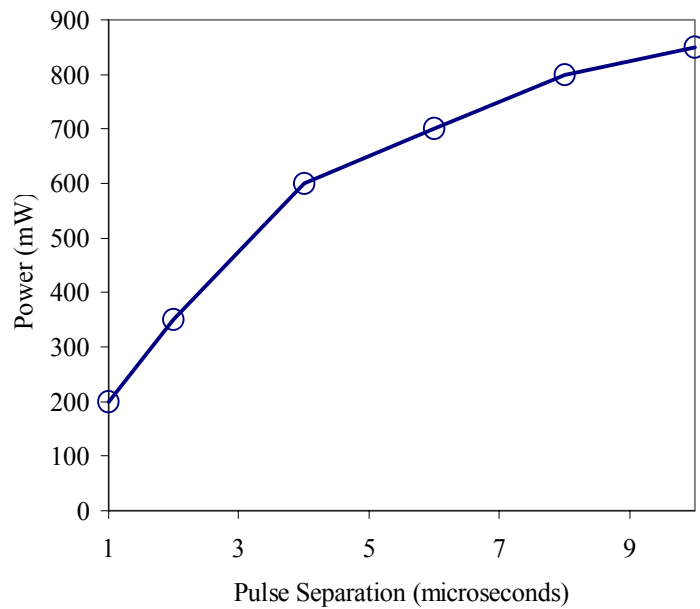


Figure 5 – Variation of laser power for a burst of 10 pulses with increasing separation between pulses.

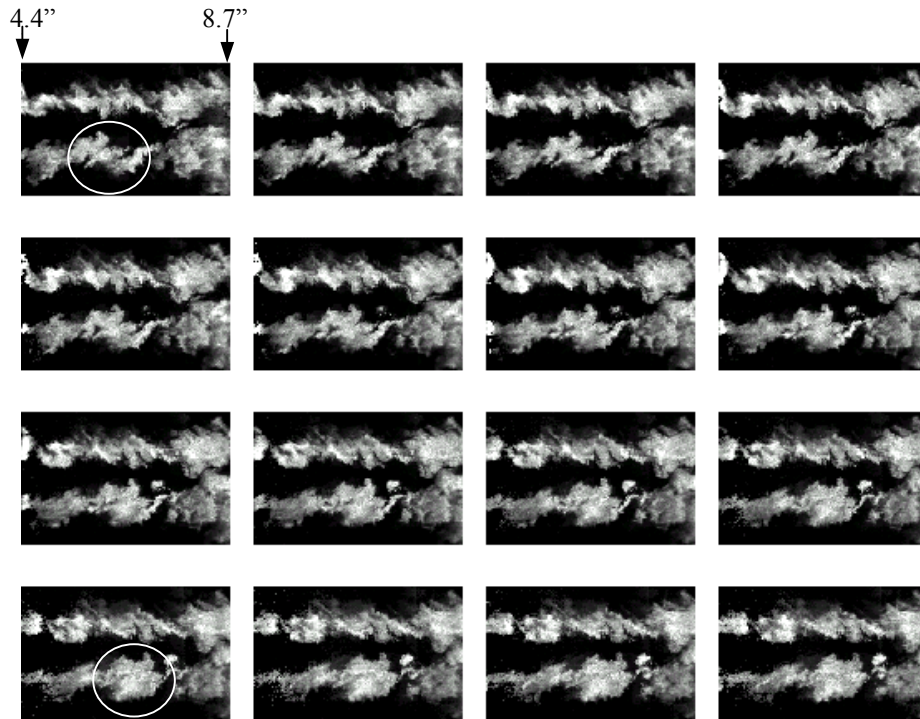


Figure 6 – Example of MHz rate imaging system. This particular example is of a structure ‘roll-up’ in the mixing layer of a Mach 1.3 axisymmetric jet. Only the mixing layer is seeded with condensed water particles from the ambient air. Flow is from left to right and images ordered left to right, top to bottom. Five microseconds separate each image. The circles indicate the region where the roll-up takes place.

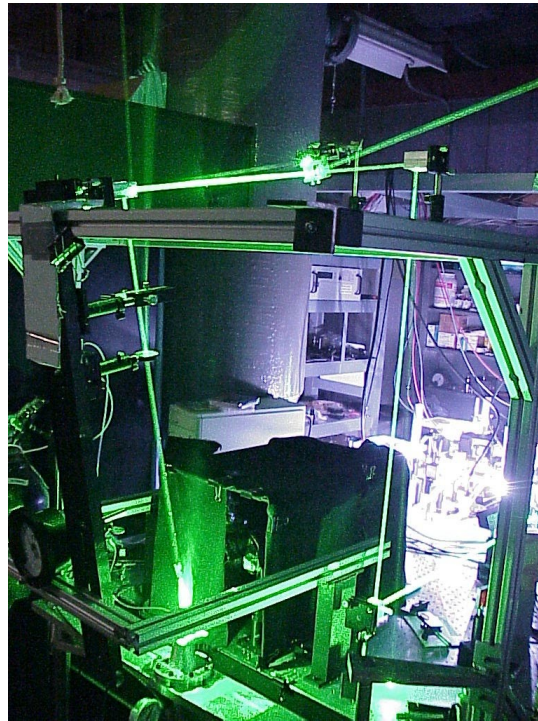


Figure 7 – Picture of real-time PDV experiment in progress. A Mach 2.0 nozzle seeded with acetone provides the flow of interest that is illuminated by the laser beam propagating down. The felt covered black cage contains the camera and filter used. The pulse burst laser is seen flashing in the background.

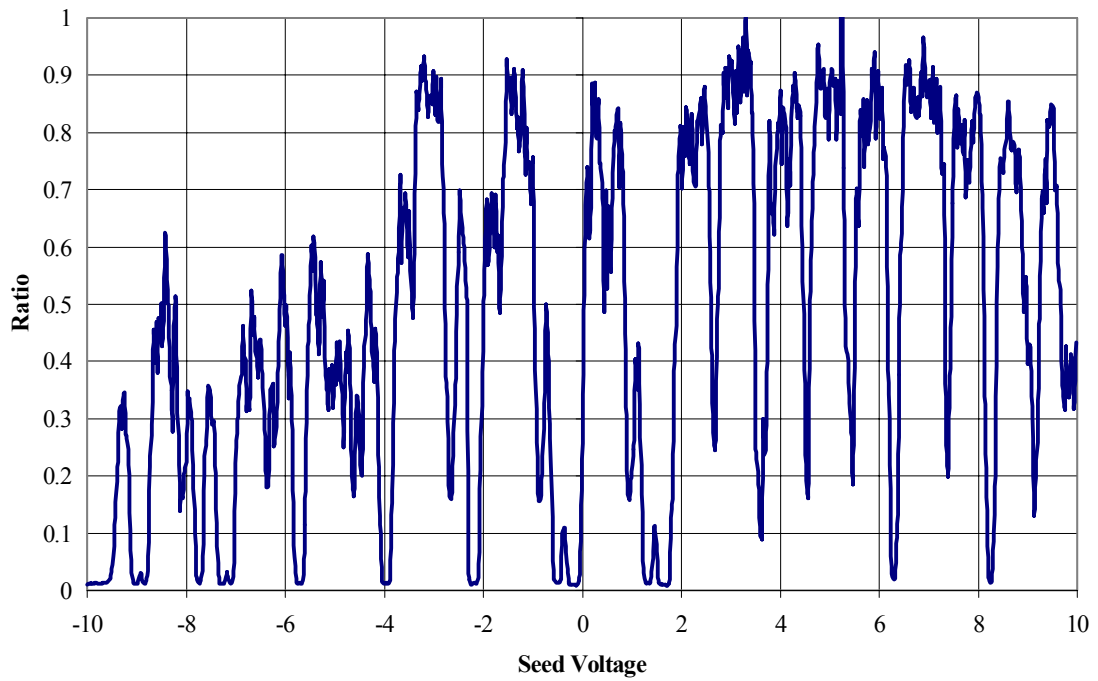


Figure 8 – Transmission of pulse burst laser beam through an iodine cell as a function of input seed voltage

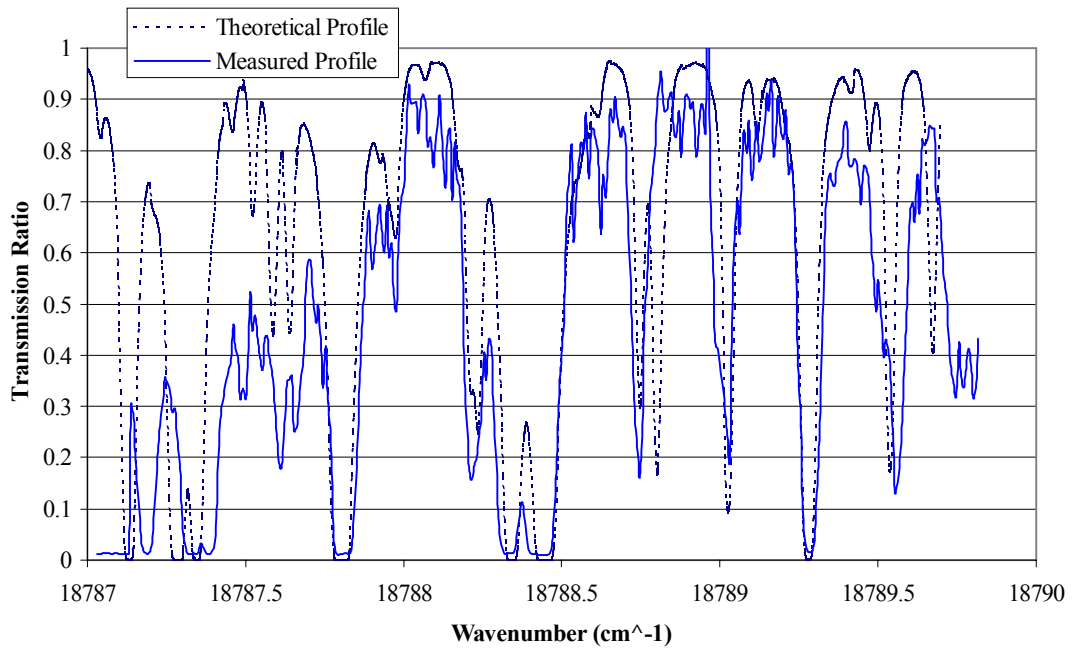


Figure 9 – Comparison of theoretical iodine spectra vs. measured iodine spectra using the pulse burst laser.

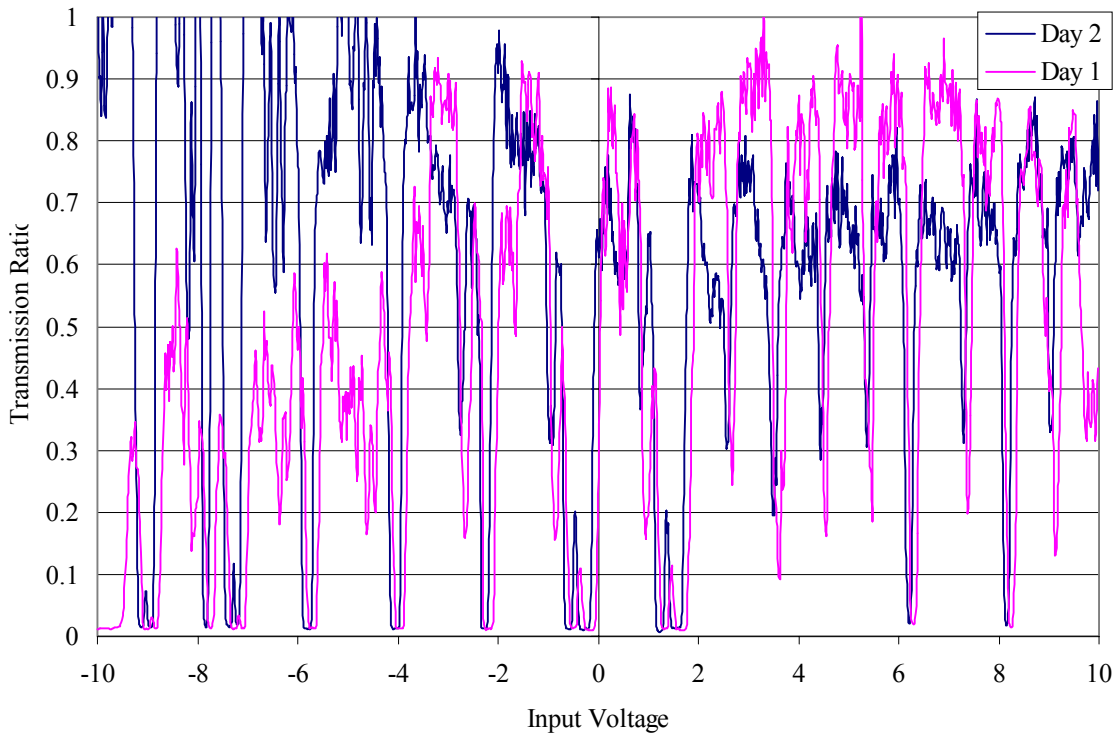


Figure 10 – Day-to-day comparison of transmission through an iodine cell by the pulse burst laser

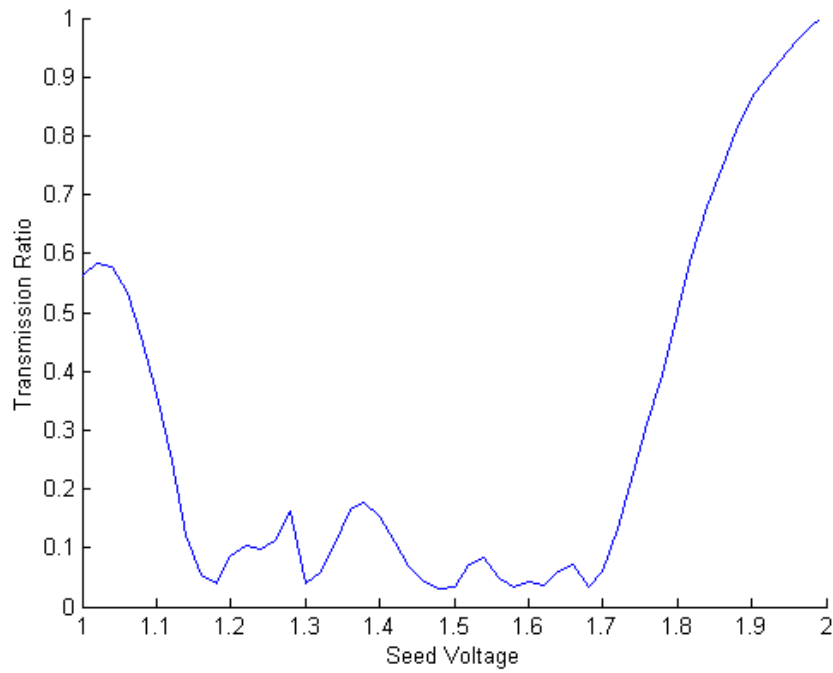


Figure 11 – Transmission profile obtained using the pulse burst laser to form a stationary spot and imaged by the SMD Camera.

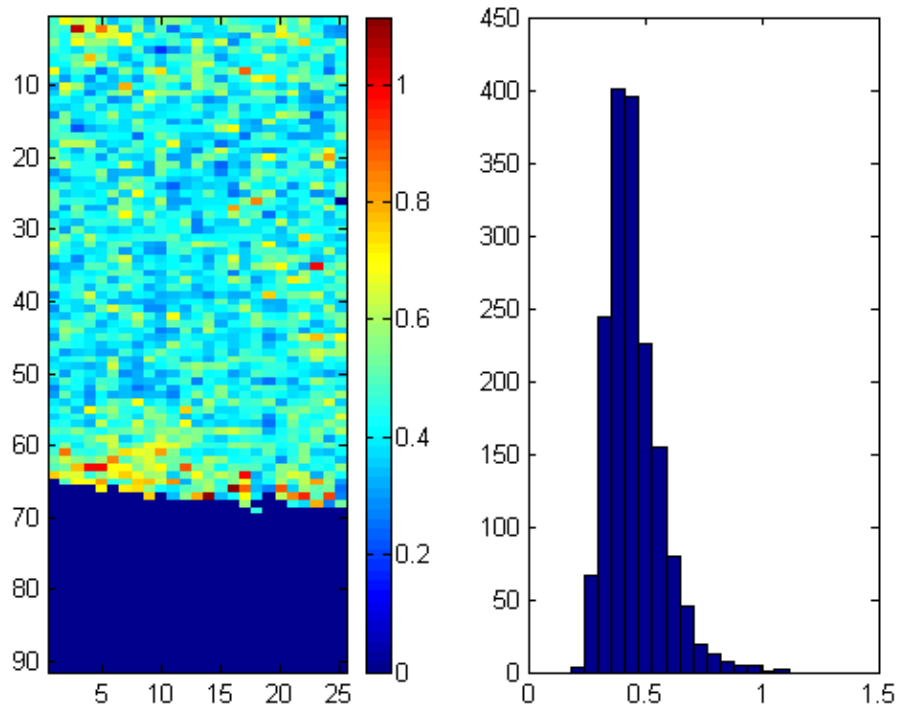


Figure 12 – Image of transmission ratios calculated for a portion of a laser beam formed into a large spot on a stationary white piece of paper and a histogram of the values. Seed voltage is held constant at 1.8 Volts.

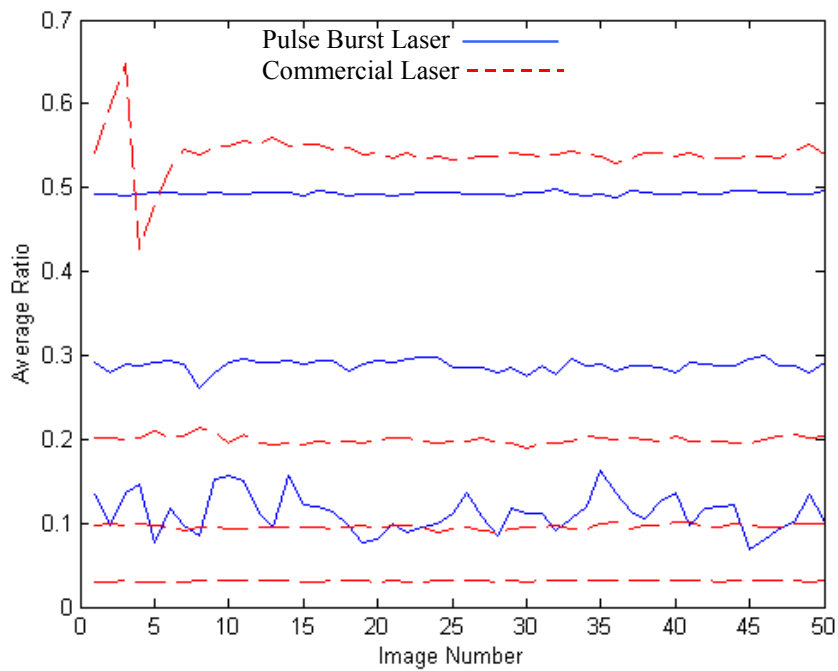


Figure 13 – Shot to Shot comparison of laser frequency. Frequency is directly proportional to the average ratio between the filtered and unfiltered images. The solid line (-) is the pulse burst laser while the dashed line (--) is a commercial Nd:YAG laser.

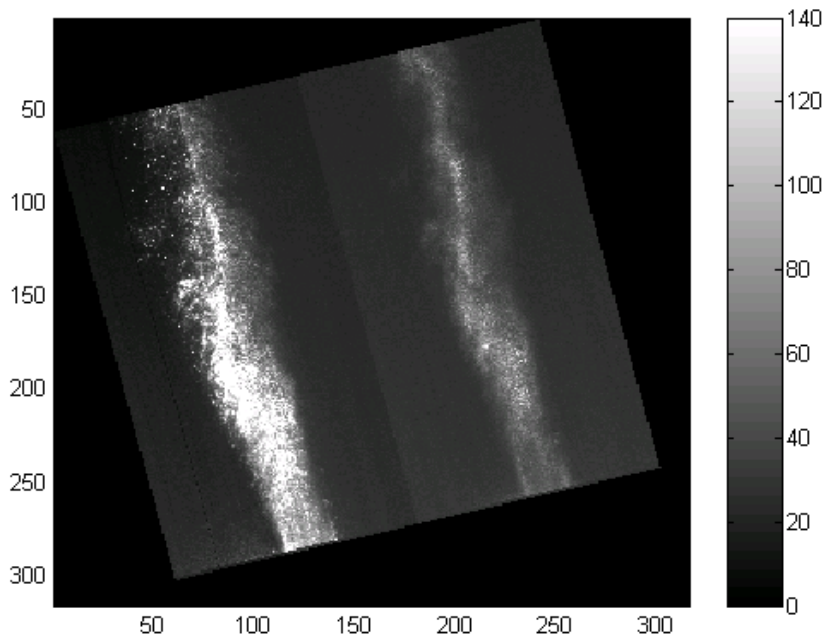


Figure 14 – Sample output from the SMD camera containing the unfiltered image on the left and the filtered image on the right.

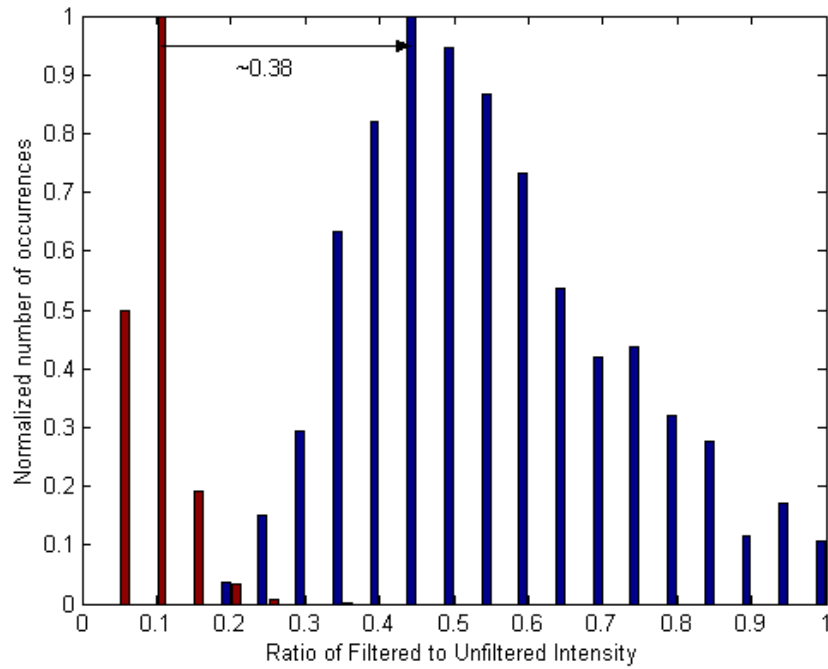


Figure 15 – Histogram of transmission ratios for Mach 2.0 nozzle as compared to a stationary target for a laser at the same frequency.